Molybdenum Cofactor Properties and [Fe-S] Cluster Coordination in *Escherichia coli* Nitrate Reductase A: Investigation by Site-Directed Mutagenesis of the Conserved His-50 Residue in the NarG Subunit†

Axel Magalon,‡ Marcel Asso,§ Bruno Guigliarelli,§ Richard A. Rothery,|| Patrick Bertrand,§ Gérard Giordano,‡ and Francis Blasco*,‡

Laboratoire de Chimie Bactérienne, IBSM, CNRS, 31 chemin Joseph Aiguier 13402 Marseille Cedex 20, France, Laboratoire de Bioénergétique et Ingénierie des Protéines, IBSM, CNRS, 31 chemin Joseph Aiguier 13402 Marseille, France, and Department of Biochemistry, 474 Medical Sciences Building, University of Alberta, Edmonton, Alberta T6G 2H7, Canada

Received November 21, 1997; Revised Manuscript Received February 11, 1998

ABSTRACT: Most of the molybdoenzymes contain, in the amino-terminal region of their catalytic subunits, a conserved Cys group that in some cases binds an [Fe-S] cluster. In dissimilatory nitrate reductases, the first Cys residue of this motif is replaced by a conserved His residue. Site-directed mutagenesis of this residue (His-50) was performed on the NarG subunit from *Escherichia coli* nitrate reductase A. The results obtained by EPR spectroscopy enable us to exclude the implication of this residue in [Fe-S] binding. Additionally, we showed that the His-50 residue does not coordinate the molybdenum atom, but its substitution by Cys or Ser introduces a perturbation of the hydrogen bonding network around the molybdenum cofactor. From potentiometric studies, it is proposed that the high-pH and the low-pH forms of the Mo(V) are both involved during the redox turnover of the enzyme. Perturbation of the Mo(V) pK_V value might be responsible for the low activity reported in the His-50−Cys mutant enzyme. A catalytic model is proposed in which the protonation/deprotonation of the Mo(V) species is an essential step. Thus, one of the two protons involved in the catalytic cycle could be the one coupled to the molybdenum atom in the dissimilatory nitrate reductase of *E. coli*.

The facultative anaerobe *Escherichia coli* develops several systems for energy generation and selects the most efficient system for a particular environment. Under anaerobic conditions and in the presence of nitrate, an electron transport chain comprising a primary dehydrogenase and the terminal membrane-bound nitrate reductase A is synthesized (*1*). The main primary dehydrogenase of this chain is believed to be the nitrate-inducible membrane-bound formate-menaquinone oxidoreductase (*2*).

Nitrate reductase A comprises a catalytic molybdenum cofactor-containing subunit (NarG; 150 kDa) (*3*), an [Fe-S] cluster-containing electron-transfer subunit (NarH; 60 kDa) (*4*, *5*) and a heme-containing membrane anchor subunit (NarI; 25 kDa) (*6*). The catalytic subunit (NarG) is a member of a family of bacterial molybdenum-containing oxidoreductase subunits with a highly conserved organization. All these subunits bind a molybdenum atom associated with a molybdopterin guanine dinucleotide cofactor (Mo-MGD). Alignment of their sequences shows extensive regions of sequence similarity throughout the length of the polypeptides (*7*−*10*). Whereas extensive studies have been done on both the NarH and the NarI subunit of the nitrate reductase A, less is known about the coordination of the molybdenum atom into the enzymatic complex.

Three classes of bacterial nitrate reductases with distinct organizations and functions have been identified according to their cellular location: the membrane-bound, the periplasmic, and the cytoplasmic enzymes. In the periplasmic enzyme, a diheme cytochrome *c* subunit, likely involved in electron transfer, is associated with the catalytic subunit (*9*, *11*). In contrast, in the cytoplasmic nitrate reductase, there is no electron-transfer subunit, but it has been proposed that [Fe-S] clusters can be bound by the molybdenum-containing subunit (*12*, *13*). Thus, despite the high identity in the primary sequences of their catalytic subunits (*8*, *9*), there may be significant differences in the structure of the molybdenum catalytic sites of the soluble and membrane-bound nitrate reductases. It has been found recently that the *Thiosphaera pantotropha* periplasmic nitrate reductase contains a [4Fe-4S] center probably bound by four cysteine residues located at the N-terminus of the catalytic subunit (*14*). The conservation of this Cys motif in the sequences of most bacterial molybdoenzymes suggests that all have a [4Fe-4S] center in their molybdenum-containing subunit (*14*, *15*). It should be noted that the first cysteine of the [Fe-S] binding motif is replaced by a histidine residue (NarG His-50) in membrane-bound nitrate reductases of various organisms (*7*, *16*, *17*). Such replacement is not inconsistent with

† This research was supported by the Centre National de la Recherche Scientifique. A.M. was supported by a fellowship from the Ministère de l'Enseignement Supérieur et de la Recherche. R.A.R. was funded by a NATO Collaborative Research Grant awarded to J.H.W.

* To whom correspondence should be addressed. Telephone: 33 (4) 91164431. Fax: 33 (4) 91718914. E-mail: blasco@ibsm.cnrs-mrs.fr.

‡ Laboratorie de Chimie Bactérienne, IBSM, CNRS.

§ Laboratorie de Bioénergétique et Ingénierie des Protéines, IBSM, CNRS.

|| University of Alberta.

S0006-2960(97)02858-4 CCC: $15.00
Published on Web 05/02/1998

[4Fe-4S] cluster coordination, as it has been recently reported in the case of the nickel−iron hydrogenase from *Desulfovibrio gigas* (*18*). However, it has been suggested that the Cys motif in the DmsA subunit from *E. coli* DMSO reductase is likely a degenerate Cys group that has lost [Fe-S] binding capability upon evolution (*10*). In such a way, the involvement of the Cys motif of the NarG subunit in [Fe-S] cluster coordination remains an open question.

Otherwise, the molybdenum cofactor (Mo(V) state) of the dissimilatory membrane-bound nitrate reductase from various organisms exhibits unique EPR properties in comparison with its periplasmic and assimilatory cytoplasmic counterparts. A key difference between the Mo(V) signals relates to the origin of the proton responsible for their hyperfine splitting. For example, the EPR Mo(V) signals from *E. coli* membrane-bound nitrate reductase undergo an acid−base transition between a low-pH and a high-pH form (*19*−*21*), the low-pH form being characterized by a strong hyperfine splitting due to a solvent-exchangeable proton (*19*, *22*). It has been proposed that only the low-pH Mo(V) form is catalytically relevant (*19*). In the *T. pantotropha* periplasmic nitrate reductase and the *Azotobacter vinelandii* assimilatory nitrate reductase, which have high-*g* split Mo(V) species, the proton is nonexchangeable and the coupling is too small to arise from a hydroxyl or thiol ligand of the Mo(V) ion (*12*, *23*). Thus, the catalytic mechanisms of the membrane-bound and of the periplasmic enzyme might be different as suggested by their different reactivities toward chlorate and azide (*11*). The highly conserved and potentially protonatable His-50 residue present in membrane-bound nitrate reductase from various organisms might be involved in defining the catalytic properties of the membrane-bound enzyme.

In this study, we have used site-directed mutagenesis to investigate the potential role(s) of NarG His-50 of the amino-terminal Cys motif (i) in ligating an [Fe-S] cluster and (ii) in the pH-dependence properties of the molybdenum of *E. coli* nitrate reductase A.

EXPERIMENTAL PROCEDURES

Bacterial Strains and Plasmids. *E. coli* LCB2048 strain (*thi-1, thr-1, leu-6, lacY1, supE44, rpsL175,* Δ(nar25(*narG-narH)*Km^r, Δ(*narU-narZ*), ΩSpec^r), Km^r) was used throughout (*24*). LCB2048 was transformed with the plasmid pVA700, which encodes the entire *narGHJI* operon under the control of the *tac* promoter (*5*). pVA700-H50C and pVA700-H50S derived from pVA700 encode for the mutated NarG[H50C]HI and NarG[H50S]HI enzymes.

Site-Directed Mutagenesis. Oligonucleotide site-directed mutagenesis was performed by overlap extension (*25*) on the pVA700 plasmid using the Expand PCR system of Boehringer as previously described (*6*).

Growth of Bacteria. Cultures were grown anaerobically at 37 °C on a minimal medium supplemented with glucose (2 g/L) and bactopeptone (2 g/L) (*5*). Isopropyl β-D-1-thiogalactopyranoside was added to a final concentration of 0.2 mM when the cell OD_{600} reached 0.3. Where appropriate, ampicillin, kanamycin, or spectinomycin was used at 50 μg/mL.

Preparation of Subcellular Fractions. The cells were harvested, washed, and resuspended in 50 mM Mops, pH 7, and 1 mM $MgCl_2$. Phenylmethanesulfonyl fluoride (0.2 mM) was added, and cells were subjected to French pressure lysis and differential centrifugation to prepare crude membrane fractions. Membranes were stored at −30 °C prior to use.

Enzyme Assays. Benzyl viologen−nitrate reductase activity was measured spectrophotometrically as previously described (*26*). One unit of nitrate reductase activity is the amount catalyzing the production of 1 μmol of nitrite min^{-1}. Quinol−nitrate reductase activities were measured spectrophotometrically according to a method adapted from Unden and Kröger (*27*) using two quinol analogues, menadiol and duroquinol (*5*, *28*).

Enzyme Titrations and EPR Spectroscopy. Redox and acid−base titrations were performed anaerobically at 21 °C, in appropriate buffers (at 50 mM), under an argon atmosphere as described in Guigliarelli et al. (*5*). Typically, the membrane preparations used for the titrations had a total protein content of about 50 mg/mL in which the proportion of nitrate reductase represented 10−20% of the total membrane protein. The preparation of samples poised at different pH was carried out by adding to a concentrated membrane solution prepared in 10 mM Mops, pH 7, a small volume of concentrated appropriate buffer (50 mM final concentration). In addition to the 100 mM Tris/HCl buffer, pH 8.3, the following buffers were used at a final concentration of 50 mM and adjusted with NaOH to the required pH: Mes (4-morpholineethanesulfonic acid), Mops (4-morpholinepropanesulfonic acid), Tricine (*N*-[2-hydroxy-1,1-bis-(hydroxymethyl)ethyl]glycine), Tris/H_2SO_4, Caps (3-cyclohexylaminopropanesulfonic acid). Phosphate and Tris buffers for which large changes of apparent pH occur on freezing (*29*) were avoided for the EPR studies of the molybdenum cofactor.

The EPR samples were taken anaerobically and quickly frozen in a cold ethanol bath. EPR spectra were recorded on a Bruker ESP300E spectrometer equipped with an Oxford Instrument ESR-900 helium-flow cryostat. Instrument conditions and temperatures are described in the individual figure captions.

RESULTS

Expression and Cellular Localization of Mutant Enzymes. The wild-type nitrate reductase A of *E. coli* is capable of supporting anaerobic respiratory growth with nitrate as the terminal electron acceptor on a glycerol−nitrate minimal medium. Substitution of His-50 with either a cysteine or a serine residue restrained or prevented strains from growing anaerobically on minimal medium (Table 1). By comparison with the wild-type enzyme, the expression of the mutant enzymes was equivalent except for the H50S mutant, which is poorly anchored to the membrane (Table 2). In all cases, the amount of overexpressed mutant enzymes was about 10 times that of the parental strain MC4100 (Table 2). The catalytic properties of wild-type nitrate reductase and mutant enzymes are compared in Table 2 using benzyl viologen as an artificial electron donor. Substitution of His-50 by a cysteine residue led to a mutant enzyme with a weak but significant activity. It is worth noting that the partition of the wild-type and H50C enzymes between the membrane and supernatant fractions, estimated from benzyl viologen−nitrate reductase activity, agreed well with that estimated by rocket immunoelectrophoresis. Substitution of His-50 with

Table 1: Nitrate Reductase Activities and Anaerobic Growth on Minimal Glycerol−Nitrate Medium

strain	menadiol−nitrate reductase activity[a]		duroquinol−nitrate reductase activity[a]		formate−nitrate reductase activity[b]	growth on minimal medium
	sp activity	%	sp activity	%		
LCB2048/pVA700	1.6	100	0.6	100	57	+++
LCB2048/pVA700 H50C	0.016	1	<0.01	ND	1.5	+/−
LCB2048/pVA700 H50S	<0.01	0	<0.01	0	0	no growth

[a] Menadiol- and duroquinol-nitrate reductase activities from membrane vesicles were measured as described in Materials and Methods and are given as (μmol of quinone formed) min^{-1} (mg of nitrate reductase)$^{-1}$ and as a percentage of the activity found in strain 2048/pVA700. [b] Formate-nitrate reductase activity was measured as previously described in Augier et al. (*26*) and is expressed in (nmol of nitrite formed) min^{-1}. ND, not determined.

Table 2: Benzyl Viologen−Nitrate Reductase Activities and Partition of Immunoprecipitated Nitrate Reductase in Membrane and Soluble Fractions of Strains Transformed with Various pVA700 Derivative Plasmids Carrying the Mutated *narG* Gene[a]

strains	immuno-precipitated nitrate reductase[a]		benzyl viologen−nitrate reductase activity		
	mg of protein	%	total activity[b]	%[c]	sp activity[d]
MC4100					
M	6	92	598	94	100
S	0.5	8	37	6	74
LCB2048/ pVA700					
M	63	97	6303	98	100
S	2	3	128	2	64
LCB2048/ pVA700 H50C					
M	54	80	26	81	0.48
S	13	20	6	19	0.46
LCB2048/ pVA700 H50S					
M	38	54	1	−	<0.05
S	32	46	0.5	−	<0.05

[a] The amount of total immunoprecipitated nitrate reductase in membrane (M) and soluble (S) fractions was expressed in mg of protein estimated by rocket immunoelectrophoresis as previously described in Augier et al. (*26*). [b] Expressed in (μmol of nitrate reduced) min^{-1}. [c] Expressed as a percentage of the sum of the activities present in the fractions. [d] Expressed in (μmol of nitrate reduced) min^{-1} (mg of nitrate reductase)$^{-1}$.

a serine residue led to the loss of the benzyl viologen−nitrate reductase activity.

Physiological Activity of Mutant Enzymes. In agreement with the inability of the mutant enzymes to support anaerobic growth on nitrate, both mutants displayed no significant activity using duroquinol or menadiol as electron donors (Table 1). Because the physiological and biochemical behavior of the mutants could result from the loss of the molybdenum cofactor (Mo-MGD), we determined the cofactor content by fluorescence assays of form A extracts (*30*). The relative amount of fluorescence detected in the form A assays for each of the enzyme preparations showed that the H50C mutant enzyme has a reduced level of molybdopterin (about 50%) compared to the wild-type enzyme (data not shown). In contrast, no molybdopterin was inserted into the H50S mutant complex, which explains the absence of any activity.

By considering the recently determined three-dimensional structure of *E. coli* formate dehydrogenase H enzyme (*36*), which contains the well-conserved Cys group at the N-terminus, it seems unlikely that the His-50 residue of NarG is close to the molybdenum atom. However, it could be possible that the substituted cysteine residue of the H50C mutant hampers the accessibility of the Mo active site to nitrate, leading to a large diminution of the catalytic activity. We therefore determined the Michaelis constant with respect to nitrate ($K_{m,nitrate}$) both in the wild-type and in the H50C mutant enzymes using benzyl viologen as electron donor. While the Michaelis constants for nitrate were comparable in the wild-type (0.12 mM) and mutant enzymes (0.07 mM), the catalytic constant (k_{cat}) in the H50C mutant (1.2 s^{-1}) is drastically affected compared to the wild-type enzyme (210 s^{-1}). Such a diminution could partly explain the lowered enzymatic activity in the H50C mutant enzyme.

EPR Studies of Wild-Type and Mutated Membrane-Bound Nitrate Reductases. EPR spectroscopy has been largely used to characterize the metal centers in wild-type and mutated nitrate reductases. To avoid spectral perturbations arising from heme−nitrosyl complexes, most of our recent works was performed on soluble enzyme (*4*, *5*, *26*, *31*). As the nitrate reduction was suspected to be responsible for the generation of iron−nitrosyl complexes (*4*), nitrate reductase was expressed from the plasmid pVA700, whose induction by isopropyl β-D-1-thiogalactopyranoside allowed us to eliminate nitrate from the growth medium. The crude membrane fractions so obtained contained high nitrate reductase concentrations, enabling EPR studies on the entire enzyme with no adventitious Fe−NO signal. These membrane fractions were titrated in Tris buffer at pH 8.3 for potentials ranging from about +300 mV to −500 mV.

At low temperature (13 K) and high microwave power (100 mW), oxidized wild-type nitrate reductase gave a typical [3Fe-4S]$^{1+}$ signal centered at $g = 1.988$ with fast relaxation properties (Figure 1a). The high field wing of this signal overlapped with an axial Mo(V) signal, which appeared at lower microwave power at $g = 1.98$ and 1.96 (see below), and was completely saturated at 100 mW. Progressive reduction of the membrane preparation led to the disappearance of the [3Fe-4S]$^{1+}$ signal, while a rhombic signal similar to that given by the highest potential [4Fe-4S]$^{1+}$ center of the soluble enzyme (center 1) increased at $g = 2.05$, 1.95, and 1.87 (Figure 1b). When the redox potential was lowered, this signal broadened slightly and an additional feature appeared at $g = 1.936$ (Figure 1c), thus revealing the reduction of a second [4Fe-4S]$^{1+}$ cluster (center 3). Below −300 mV, a peak increased strongly at $g = 1.916$ and the EPR spectrum became very broad (Figure 1d,e), which denotes the reduction of a third [4Fe-4S] center (center 4) magnetically coupled to the other clusters. The spectral properties of the membrane-bound nitrate reductase appear to be very similar to those of the soluble enzyme (*26*), except for the [3Fe-4S]$^{1+}$ signal which showed a more prominent

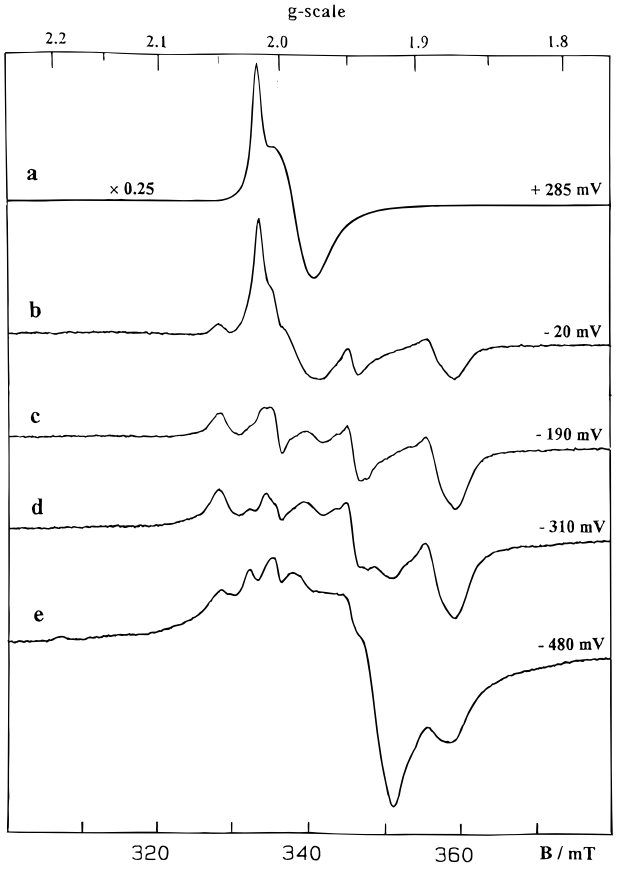

FIGURE 1: Representative EPR spectra obtained during the redox titration of the wild-type membrane-bound nitrate reductase. Experimental conditions: temperature, 13 K; microwave frequency, 9.333 GHz; microwave power, 100 mW; modulation amplitude, 0.5 mT.

shoulder at $g = 2.00$ (*32*). This asymmetrical line shape is reminiscent of that usually observed in ferredoxins (*33*) and suggests that the NarGH complex undergoes some conformational changes upon its insertion into the membrane. This is supported by the variations of the interaction spectrum given by the fully reduced enzyme in the soluble and membrane-bound forms. However, as these spectral features are very sensitive to structural variations, such conformational changes are expected to be weak.

EPR titrations of membrane fractions containing the mutated nitrate reductases H50C (Figure 2) and H50S (Figure 3) were performed using the same conditions as for the wild-type enzyme. Over the potential range studied, the EPR spectra of both mutants were very similar to those given by the wild-type enzyme (Figure 1). Only minor line shape variations were found for the interaction spectra given by the fully reduced enzymes (Figures 2e and 3e), likely arising from small changes of the relative arrangement of the clusters. The saturation properties of the [Fe-S] signals were found to vary slightly between the wild-type and the mutant enzymes, which precludes comparison of the [Fe-S] content of the enzyme from simple amplitude measurements at 100 mW. Spin-intensity measurements performed in nonsaturating conditions (1 mW microwave power) or corrected to take into account saturation effects gave an intensity ratio of 1:3 (±20%) between the fully oxidized and the fully dithionite-reduced forms of the wild-type and mutated nitrate reductase. If one considers that nitrate reductase contains one [3Fe-4S] center per molecule, this confirms the presence of three

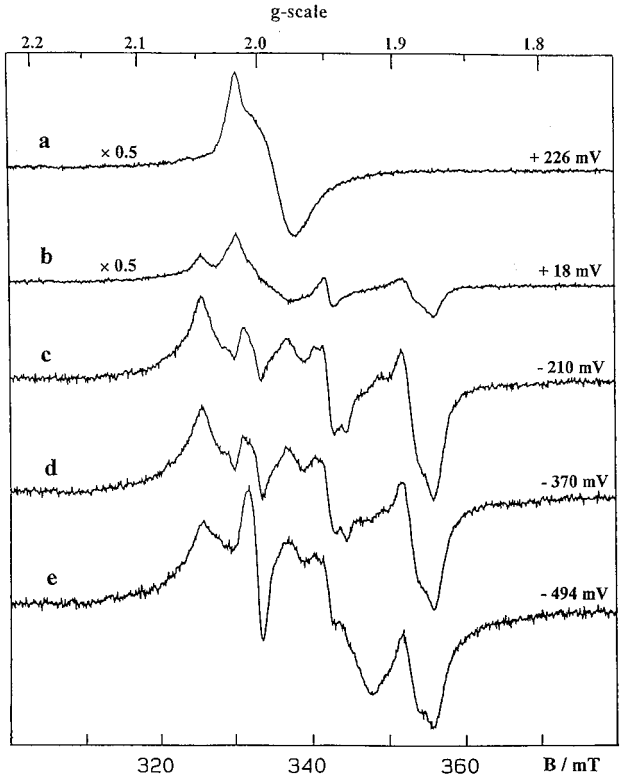

FIGURE 2: Representative EPR spectra obtained during the redox titration of the mutated NarG[H50C]HI membrane-bound nitrate reductase. Experimental conditions were as described in Figure 1.

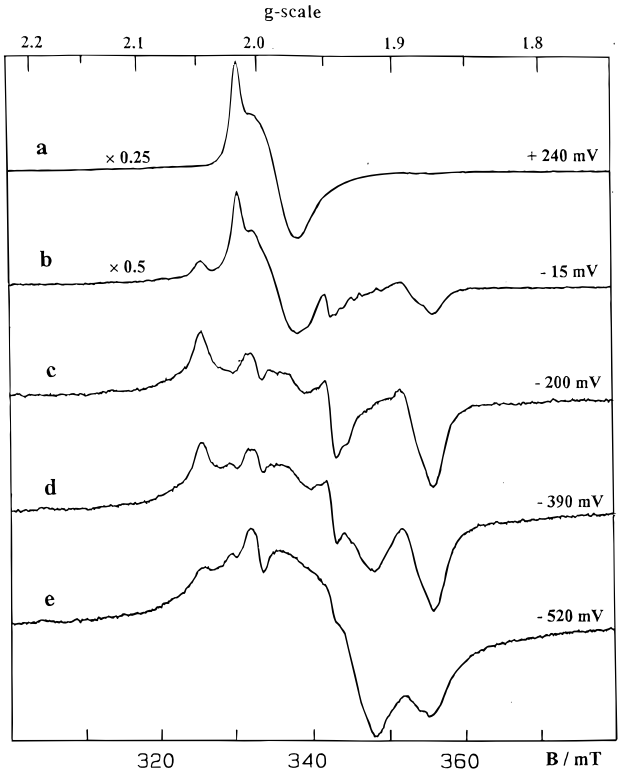

FIGURE 3: Representative EPR spectra obtained during the redox titration of the mutated NarG[H50S]HI membrane-bound nitrate reductase. Experimental conditions were as in Figure 1, except for the microwave frequency, 9.421 GHz.

[4Fe-4S] clusters in the mutated enzymes and strongly indicates that, in both cases, the His 50 replacements did not affect the insertion of the [Fe-S] clusters. Furthermore, these intensity measurements gave no evidence for the

Table 3: Midpoint Potentials of the Iron−Sulfur Centers in the Wild-Type and Mutated Nitrate Reductases from *E. coli*

strains	midpoint potentials (mV)[a] center 1, [4Fe-4S]	center 2, [3Fe-4S]	center 3, [4Fe-4S]	center 4, [4Fe-4S]
MC4100[b]	+60 (+80)[c]	+20 (+60)[c]	−200	−400
LCB79/pVA7 + pVA50[d]	+90	+20	nd	nd
LCB2048/pVA700[e]	+30	+50	−80	−410
LCB2048/pVA700-H50C[e]	+20	+50	−70	−390
LCB2048/pVA700-H50S[e]	−10	+30	−80	−350

[a] Midpoint potentials measured in Tris buffer, pH 8.3. [b] Heat-solubilized nitrate reductase, from Guigliarelli et al. (*4*). [c] Microscopic redox potentials deduced by taking into account the anticooperative redox interaction between centers 1 and 2. [d] Soluble enzyme, from Augier et al. (*26*). [e] Membrane-bound nitrate reductase, this work. The uncertainty on the potential values is ± 10 mV. nd: not determined.

generation of a fourth [4Fe-4S] cluster by the H50C or H50S mutations in the 800 mV potential range investigated.

The redox properties of the different clusters were determined by monitoring, as a function of the potential, the peak amplitudes at $g = 2.02$ for the [3Fe-4S] center and at $g = 1.87$, 1.936, and 1.916 for the three [4Fe-4S] clusters (centers 1, 3, and 4, respectively). These amplitude variations were fitted to Nernstian curves, and the corresponding midpoint potentials are reported in Table 3. As in the soluble enzyme, the redox behavior of the two highest potential clusters showed a slight departure from a Nernstian curve, which was previously interpreted as arising from anticooperative redox interactions (*4*, *26*). By comparison with soluble nitrate reductase (Table 3; refs *4* and *26*), the [Fe-S] centers of the membrane-bound enzyme kept their redox potential values in the same range, except for center 3 for which the potential was shifted by about +120 mV in membranes (Table 3).

The EPR spectra of the membrane-bound enzymes were also examined at higher temperature (50 K). Under these conditions, the [Fe-S] signals were completely broadened by relaxation effects, thus enabling an accurate study of the molybdenum cofactor signals. In the oxidized states of the wild-type and H50C nitrate reductases, a nearly axial Mo(V) signal at $g = 1.987$, 1.981, and 1.962, which is identical to the high pH Mo(V) signal of the soluble enzyme (*19*), was observed (Figure 4 a,d). In both cases, the amplitude of this signal showed a bell-shaped variation as a function of the redox potential with a maximum at about +125 mV, as in the soluble enzyme in the same Tris buffer (*4*). When these variations were fitted with theoretical curves corresponding to two successive one-electron redox processes, the midpoint potentials of the Mo(IV)/Mo(V) and Mo(V)/Mo(VI) couples in Tris buffer (pH 8.3) were found to be 0 and +250 mV for the wild-type enzyme and +40 and +200 mV for the H50C enzyme (data not shown). In contrast, no Mo(V) EPR signal could be detected in the H50S mutant, which is consistent with the fluorescence experiments showing that the molybdopterin is not incorporated in this enzyme.

The Mo(V) EPR signal of nitrate reductase is well-known to undergo a low-pH/high-pH transition (*19*). To study this acid−base process in membrane-bound enzymes, oxidized preparations of membrane fractions containing either the wild-type or the H50C mutant protein were titrated as a

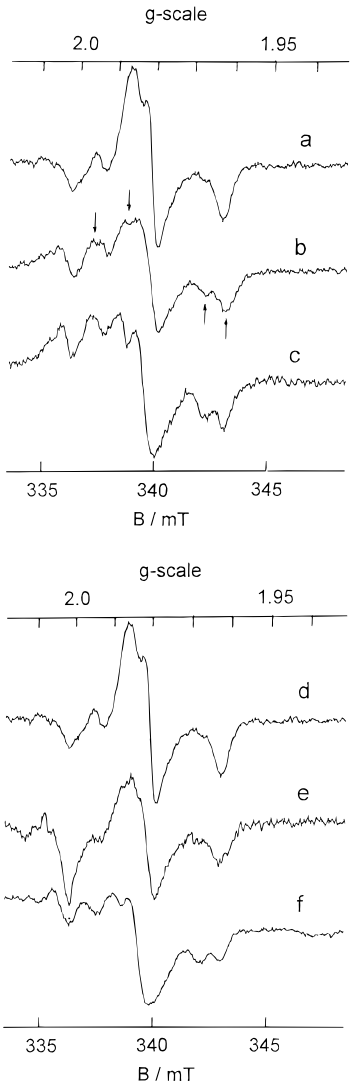

FIGURE 4: Effect of pH on the molybdenum (V) EPR signal of the wild-type and mutated membrane-bound nitrate reductases. (a−c) Wild-type enzyme; (d−f) NarG[H50C]HI mutant. The buffers were (a, d) tricine, pH 8.1; (b, e) Mops, pH 7.1; and (c) Mes, pH 5.65 and (f) 5.85. EPR conditions: temperature, 50 K; microwave frequency, 9.421 GHz; microwave power, 4 mW; modulation amplitude, 0.4 mT.

function of pH and investigated by EPR. Great care was taken to avoid buffers which undergo pH shifts upon freezing (*29*) and to avoid anions expected to affect the protonation process (*34*, *35*). The acid−base interconversion was observed for both enzymes, and the low-pH Mo(V) signal split by proton hyperfine interactions was similar to that given by the soluble enzyme (Figure 4c,e). By measuring the amplitudes of the lines belonging to the high-pH and low-pH signals, respectively (see arrows in Figure 4), the proportion of the low-pH Mo(V) species was determined for each studied pH (Figure 5). Owing to a progressive denaturation of these enzymes in acidic conditions, these measurements were limited to pH > 5.5. The results showed clearly that the H50C mutation induced a shift from 7.4 to 6.8 for the pK_V value of the acid−base interconversion of the Mo(V) signal (Figure 5). The redox properties of the two acid−base forms of the molybdenum cofactor were then investigated by carrying out EPR redox titrations of the enzyme in tricine at pH 8.1 and in Mes at pH 5.85 for which pure high-pH or low-pH Mo(V) signals could be observed,

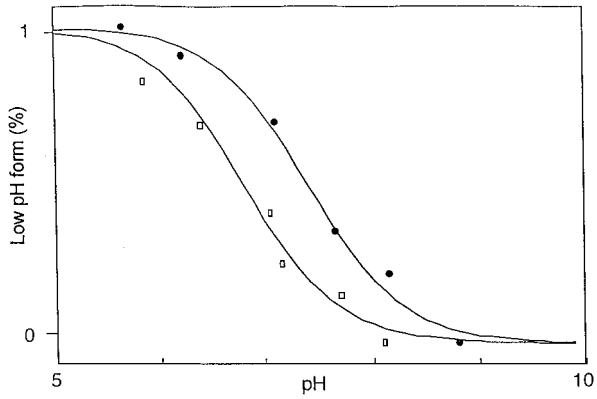

FIGURE 5: Percentage of the low-pH form in the Mo(V) EPR signal as a function of pH. The percentage of the low-pH EPR signal was deduced from peak amplitude measurements as indicated in the text. (●) Wild-type membrane-bound nitrate reductase; (□) mutated NarG[H50C]HI membrane-bound nitrate reductase. The solid lines are the theoretical dissociation curves calculated for an acid with a pK_V of 7.4 and 6.8, respectively.

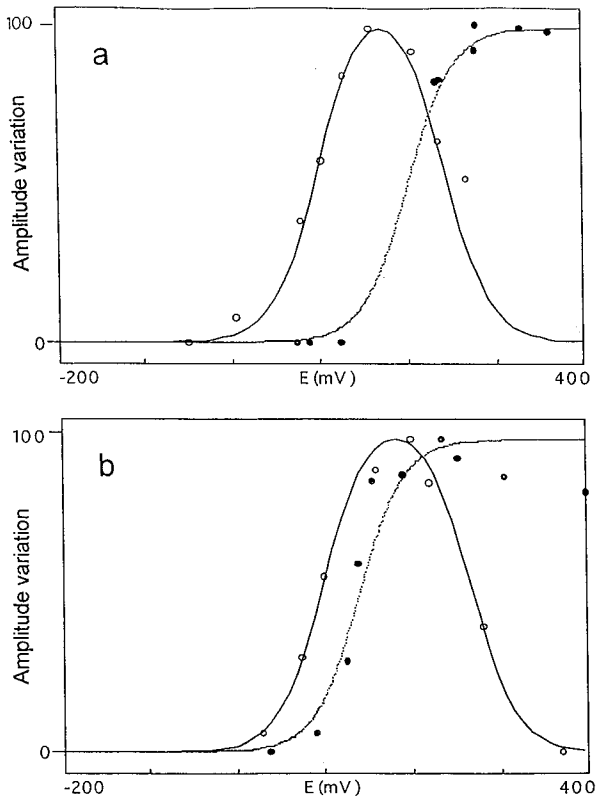

FIGURE 6: Normalized amplitude variations of the Mo(V) EPR signals as a function of the redox potential in membrane-bound nitrate reductases. (a) wild-type enzyme, (b) NarG[H50C]HI mutant. Experimental conditions were as described in Figure 4. Peak to peak amplitudes were measured at $g = 1.981$ for the high-pH signal in a redox titration carried out in tricine, pH 8.1 (○), and at $g = 1.983$ for the low-pH signal in a redox titration carried out in Mes, pH 5.85 (●). Solid lines result from Nernst plots with the midpoint potentials given in Table 4.

respectively. Surprisingly, whereas bell-shaped variations were observed for the high-pH Mo(V) signal amplitude in both the wild-type and the H50C enzyme, no oxidation of the low-pH Mo(V) form was found in the studied potential range (Figure 6). This indicates that the redox potential of the Mo(V)/Mo(VI) couple undergoes a considerable positive shift in the low-pH form. The midpoint potentials of the other molybdenum redox couples were determined as

Table 4: Midpoint Potentials of the Molybdenum Cofactor in the Wild-Type and Mutated Membrane-Bound Nitrate Reductases from *E. coli*

		midpoint potentials (mV)[a]	
strains	buffers	Mo(IV)/ Mo(V)	Mo(V)/ Mo(VI)
LCB2048/pVA700	Tricine, pH 8.1	$E_1 = +90$	$E_2 = +250$
	Mes, pH 5.85	$E_3 = +200$	$E_4 > +450$
LCB2048/pVA700-H50C	Tricine, pH 8.1	$E_1 = +100$	$E_2 = +280$
	Mes, pH 5.85	$E_3 = +130$	$E_4 > +450$

[a] The uncertainty on the potential values is ±10 mV.

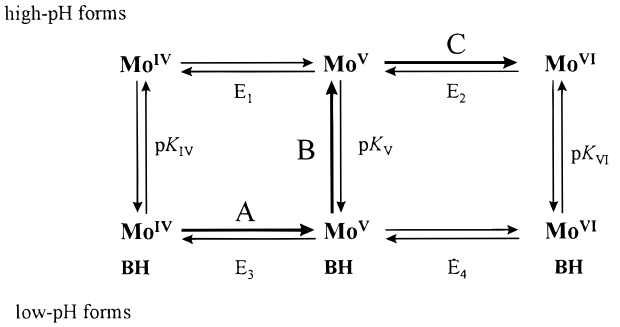

FIGURE 7: Schematic representation of the acid−base and redox equilibria involved between the low-pH and high-pH forms of the molybdenum cofactor in *E. coli* nitrate reductase. In the wild-type enzyme, the p*K* values are the following: p$K_{IV} = 9.3$, p$K_V = 7.4$, and p$K_{VI} < 4.1$. In the H50C mutant enzyme, the p*K* values are the following: p$K_{IV} = 7.3$, p$K_V = 6.8$, and p$K_{VI} < 4.0$. B corresponds to the base whose protonation leads to the low-pH Mo(V) signal.

indicated above (Table 4), and the relations between the various states of the molybdenum cofactor are summarized in Figure 7. In this scheme, the acid−base properties of the Mo(IV) and Mo(VI) redox states can be simply deduced from the values of pK_V and of the various redox potentials by the following expressions: $pK_V - pK_{VI} = (E_4 - E_2)/58$, and $pK_{IV} - pK_V = (E_3 - E_1)/58$, with E_i in millivolts. By using the values given in Table 4, we found p$K_{IV} = 9.3$ and p$K_{VI} < 4.1$ for the wild-type nitrate reductase, and p$K_{IV} = 7.3$ and p$K_{VI} < 4.0$ for the H50C mutant.

DISCUSSION

The amino-terminal region of most catalytic subunits of multimeric respiratory molybdoenzymes contains a Cys group of the form $CX_{2-3}CX_3CX_{26-34}C$, with the exception, however, of the NarG subunit from nitrate reductase A where a His residue replaces the first Cys residue of the motif. It has been tempting to speculate that these Cys groups are involved in ligating an additional [Fe-S] center. In this report, the His residue of the Cys group of NarG was mutated to a Cys or Ser residue so that the modified Cys motif could bind a new [Fe-S] cluster or modify the physicochemical properties of an existing cluster. However, the EPR spectra of membranes containing NarG mutant enzymes were found to be essentially identical to those of the wild-type enzyme. All four previously characterized [Fe-S] clusters are present in the mutant enzymes with midpoint potentials similar to those of the wild-type enzyme (Table 3). Although we cannot absolutely exclude the existence in the NarG subunit of an [Fe-S] center with a very low midpoint potential ($E_{m,8.3}$

< -600 mV), these results are consistent with our previous site-directed mutagenesis studies done on the soluble enzyme (*5*) and enable us to conclude that the four EPR-visible [Fe-S] clusters are all ligated by the Cys groups of NarH.

Recently, the structures of several sequence-related molybdenum-containing enzymes have been determined by X-ray crystallography (*36*, *38*, *39*, *40*). From these studies a similar polypeptide fold and active site has begun to emerge among several molybdoenzymes. Furthermore, it has been shown recently, in the crystal structure of formate dehydrogenase H, which displays high sequence similarity with nitrate reductase A, that the region surrounding the amino-terminal [Fe-S] binding motif is located just below the protein surface and close to the molybdopterin (*36*). Mutational analysis of this motif in DmsA of the DMSO reductase from *E. coli* reveals that while these Cys residues are important for electron transfer within the enzymatic complex, they do not ligate an EPR-visible iron−sulfur cluster (*37*). One possible reason for the difference between the FdhF protein and both the DmsA and the NarG protein in the [4Fe-4S] cluster coordination may reside in the relative geometry of the Cys groups (*10*). NarG and DmsA proteins have three residues between the first two Cys residues instead of two as in the Cys motif of other bacterial molybdoenzyme proteins, and these differences might drastically alter the ability of the Cys group to direct cluster formation in both DmsA and NarG subunits.

Although the His-50 residue is apparently not involved in iron−sulfur cluster coordination, its substitution by Ser or Cys unexpectedly causes significant perturbation of the molybdenum cofactor. As shown by fluorescence analysis of the pterin content and the EPR spectrum analysis, the H50S mutation leads to the loss of the molybdenum cofactor, resulting in an inactive enzyme. In contrast, the molybdenum cofactor is present in a large proportion of the H50C mutant enzyme. However, the resulting mutant strain cannot support growth on nitrate under anaerobic conditions, and the mutant enzyme exhibits reduced $BV^{\bullet+}$ oxidase as well as quinol oxidase activities.

In an earlier study, the EPR properties of the molybdenum center of nitrate reductase A were investigated by Vincent and co-workers, who identified a low-pH and a high-pH form of the Mo(V) EPR signal (*19*). In the presence of added chloride, these forms represent a conjugate acid/base pair with a pK_V of 8.26 in the detergent-solubilized form of the enzyme (*19*). Initially, these authors had suggested that only the low-pH form of the Mo(V) is catalytically competent since the enzymatic activity exhibits a comparable pH profile, with the enzyme rapidly losing its activity above pH 8.5 (*19*). However, it has been subsequently shown that binding of anions such as chloride to the molybdenum atom in nitrate reductase A modifies the apparent pK_V for the high-pH/low-pH transition, which brought into question the actual role of the two Mo(V) species (*34*, *35*). Moreover, it has been proposed that the transition between the low-pH and the high-pH form of the Mo(V) might be triggered by the protonation of the protein rather than by the protonation of a molybdenum ligand (*34*). The conserved His-50 residue, which is only present in membrane-bound nitrate reductases, appears as a potential candidate for such an acid−base process. Hence, we have carefully studied the molybdenum cofactor properties in the wild-type and His-50 mutated enzymes. Substitution of His-50 with Cys does not lead to modification of the *g* values of the two EPR forms of the Mo(V) signal. This result clearly indicates that the His-50 residue does not coordinate the molybdenum atom. This is in agreement with the three-dimensional structure of the *E. coli* formate dehydrogenase H enzyme showing that the homologous residue and the Mo atom are on the opposite sides of a pterin of the Mo-(bis-MGD) cofactor (*36*). The EPR spectral analysis of the membrane-bound enzymes shows that the two Mo(V) forms represent a conjugate acid/base pair with a pK_V of 7.4 in the wild-type enzyme, in the absence of added chloride. Under the same conditions, the pK_V is 6.8 in the H50C mutant enzyme. Such a pK_V shift could result from a perturbation of the hydrogen bonding network around the molybdenum atom leading to an indirect effect on its protonation. The His-50 residue is most likely involved in stabilization of the hydrogen bonding network of the molybdenum cofactor, since in the H50S mutant enzyme the replacement of a sulfydryl group by a hydroxyl one is sufficient to preclude the binding of the molybdenum cofactor.

To gain further insights into the functional significance of the different Mo(V) species, comparative potentiometric studies of both the low-pH and the high-pH form of Mo(V) in the wild-type and mutant enzymes were performed. At high pH, similar midpoint values were found for the Mo(VI)/(V) and Mo(V)/Mo(IV) couples between the wild-type and H50C mutant enzymes (Table 4). Surprisingly, at low pH, no oxidation of the Mo(V) state to the Mo(VI) state was observed even at potentials as high as +400 mV, which shows that the midpoint potential of the low-pH Mo(V)/Mo(VI) couple is significantly higher than this value. In contrast to what has been previously suggested (*19*), this indicates that the low-pH form of the Mo(V) cannot be the only catalytically active Mo(V) species during the enzyme turnover. Indeed, the inability of the low-pH Mo(V) form to undergo final oxidation to Mo(VI) would prevent the reduction of nitrate to nitrite ($E_{m,7} = +420$ mV), a two-electron and two-proton process. Overall, these results lead us to propose that the high-pH and the low-pH form of the Mo(V) are both involved during the redox turnover of the enzyme. While no evidence has been reported indicating that the high-pH Mo(V) species binds nitrate, it has been shown that the low-pH Mo(V) species is able to bind it (*23*). By considering that the Mo potentials are not strongly affected by nitrate binding, these results together with those obtained in the present study suggest the following model for the reoxidation of the molybdenum atom by nitrate during the catalytic cycle. The first one-electron reoxidation step of the low-pH Mo(IV) species leads to the low-pH Mo(V) form (Figure 7, step A). Deprotonation occurs at the active site, according to the pK_V value, yielding the high-pH Mo(V) form (Figure 7, step B). The second one-electron reoxidation step leads to nitrite and the Mo(VI) species (Figure 7, step C). One of the key features of this model is that one of the two protons involved in the nitrate reduction might be the one associated with the acid−base transition of the molybdenum cofactor. Modification of the pK_V value in the H50C mutant enzyme changes the interconversion rate between the low-pH and high-pH forms of the Mo(V), which as a consequence could affect the rate of the catalytic cycle.

An alternative explanation for such a lowered activity would be that the enzyme affinity for nitrate is modified in the H50C mutant enzyme. A common feature of the molybdoenzymes with known three-dimensional structure is the location of the active site at the bottom of a large depression in the protein surface resembling a funnel where only the Mo atom and three of the coordinating sulfur ligands are accessible from the solvent (*36*, *38*, *39*, *40*). The presence of bulky side chains of charged residues has been suggested to modulate the access to the active site and serve as a lid when necessary (*36*, *38*). In the case of the H50C substitution, we have shown that the very low activity is not related to alteration of the Michaelis constant for nitrate, thus excluding a bulk effect of the Cys residue at or near the access funnel to the active site, and this is consistent with our model.

In the model described herein, one of the two protons involved in reduction of nitrate to nitrite is missing. This proton could be provided by a protonatable amino acid residue lying in the vicinity of the molybdenum cofactor. For example, it has been proposed that His-141 could constitute such a proton donor during the catalytic cycle in the *E. coli* formate dehydrogenase H (*36*, *41*).

Finally, our work suggests that the proton-transfer mechanism associated with the nitrate reduction could be different between the membrane-bound and the periplasmic nitrate reductases. It is worth noting that the high-*g* split signal of the Mo(V) from the periplasmic nitrate reductase of *T. pantotropha*, which has been suggested to be physiologically relevant, exhibits a small coupling with a nonexchangeable proton (*23*). Moreover, addition of various anions such as nitrate and chloride failed to modify this EPR signal (*23*), contrary to what is observed in membrane-bound nitrate reductases (*34*, *35*). It is unlikely that the nonexchangeable proton coupled to the molybdenum cofactor is involved in nitrate reduction in the former enzyme. Site-directed mutagenesis on conserved protonatable residues in the NarG sequence of the membrane-bound nitrate reductase of *E. coli* is in progress in our laboratory to define those involved in the catalytic reaction.

REFERENCES

1. Pichinoty, F. (1969) *Arch. Microbiol. 68*, 51−64.
2. Berg, B. L., Li, J., Heider, J., and Stewart, V. (1991) *J. Biol. Chem. 266*, 22380−22385.
3. DerVartanian, D. V., and Forget, P. (1975) *Biochim. Biophys. Acta 379*, 74−80.
4. Guigliarelli, B., Asso, M., More, C., Augier, V., Blasco, F., Pommier, J., Giordano, G., and Bertrand, P. (1992) *Eur. J. Biochem. 207*, 61−68.
5. Guigliarelli, B., Magalon, A., Asso, M., Bertrand, P., Frixon, C., Giordano, G., and Blasco, F. (1996) *Biochemistry 35*, 4828−4836.
6. Magalon, A., Lemesle-Meunier, D., Rothery, R. A., Frixon, C., Weiner, J. H., and Blasco, F. (1997) *J. Biol. Chem. 272*, 25652−25658.
7. Blasco, F., Iobbi, C., Ratouchniak, J., Bonnefoy, V., and Chippaux, M. (1990) *Mol. Gen. Genet. 222*, 104−111.
8. Wootton, J. C., Nicolson, R. E., Cock, J. M., Walters, D. E., Burke, J. F., Doyle, W. A., and Bray, R. C. (1991) *Biochim. Biophys. Acta 1057*, 157−185.
9. Berks, B. C., Ferguson, S. J., Moir, J. W., and Richardson, D. J. (1995) *Biochim. Biophys. Acta 1232*, 97−173.
10. Trieber, C. A., Rothery, R. A., and Weiner, J. H. (1996) *J. Biol. Chem. 271*, 4620−4626.
11. Berks, B. C., Richardson, D. J., Robinson, C., Reilly, A., Aplin, R. T., and Ferguson, S. J. (1994) *Eur. J. Biochem. 220*, 117−124.
12. Gangeswaran, R., Lowe, D. J., and Eady, R. R. (1993) *Biochem. J. 289*, 335−342.
13. Lin, J. T., Goldman, B. S., and Stewart, V. (1993) *J. Bacteriol. 175*, 2370−2378.
14. Breton, J., Berks, B. C., Reilly, A., Thomson, A. J., Ferguson, S. J., and Richardson, D. J. (1994) *FEBS Lett. 345*, 76−80.
15. Berks, B. C., Page, M. D., Richardson, D. J., Reilly, A., Cavill, A., Outen, F., and Ferguson, S. J. (1995) *Mol. Microbiol. 15*, 319−331.
16. Blasco, F., Iobbi, C., Giordano, G., Chippaux, M., and Bonnefoy, V. (1989) *Mol. Gen. Genet. 218*, 249−256.
17. Hoffmann, T., Troup, B., Szabo, A., Hungerer, C., and Jahn, D. (1995) *FEMS Microbiol. Lett. 131*, 219−225.
18. Volbeda, A., Charon, M. H., Piras, C., Hatchikian, E. C., Frey, M., and Fontecilla-Camps, J. C. (1995) *Nature 373*, 580−587.
19. Vincent, S. P., and Bray, R. C. (1978) *Biochem. J. 171*, 639−647.
20. Sears, H. J., Bennett, B., Spiro, S., Thomson, A. J., and Richardson, D. J. (1995) *Biochem. J. 310*, 311−314.
21. Godfrey, C., Greenwood, C., Thomson, A. J., Bray, R. C., and George, G. N. (1984) *Biochem. J. 224*, 601−608.
22. Turner, N., Ballard, A. L., Bray, R. C., and Ferguson, S. (1988) *Biochem. J. 252*, 925−926.
23. Bennett, B., Berks, B. C., Ferguson, S. J., Thomson, A. J., and Richardson, D. J. (1994) *Eur. J. Biochem. 226*, 789−798.
24. Blasco, F., Nunzi, F., Pommier, J., Brasseur, R., Chippaux, M., and Giordano, G. (1992) *Mol. Microbiol. 6*, 209−219.
25. Ho, S. N., Hunt, H. D., Horton, R. M., Pullen, J. K., and Pease, L. R. (1989) *Gene 77*, 51−59.
26. Augier, V., Guigliarelli, B., Asso, M., Bertrand, P., Frixon, C., Giordano, G., Chippaux, M., and Blasco, F. (1993) *Biochemistry 32*, 2013−2023.
27. Unden, G., and Kroger, A. (1986) *Methods Enzymol. 126*, 387−399.
28. Giordani, R., Buc, J., Cornish-Bowden, A., and Cardenas, M.-L. (1997) *Eur. J. Biochem. 250*, 567−577.
29. Williams-Smith, D. L., Bray, R. C., Barber, M. J., Tsopanakis, A. D., and Vincent, S. P. (1977) *Biochem. J. 167*, 593−600.
30. Johnson, J. L., Indermaur, L. W., and Rajagopalan, K. V. (1991) *J. Biol. Chem. 266*, 12140−12145.
31. Augier, V., Asso, M., Guigliarelli, B., More, C., Bertrand, P., Santini, C. L., Blasco, F., Chippaux, M., and Giordano, G. (1993) *Biochemistry 32*, 5099−5108.
32. Magalon, A., Rothery, R. A., Giordano, G., Blasco, F., and Weiner, J. H. (1997) *J. Bacteriol. 179*, 5037−5045.
33. Guigliarelli, B., More, C., Bertrand, P., and Gayda, J.-P. (1986) *J. Chem Phys. 85*, 2774−2778.
34. George, G. N., Bray, R. C., Morpeth, F. F., and Boxer, D. H. (1985) *Biochem. J. 227*, 925−931.
35. George, G. N., Turner, N. A., Bray, R. C., Morpeth, F. F., Boxer, D. H., and Cramer, S. P. (1989) *Biochem. J. 259*, 693−700.
36. Boyington, J. C., Gladyshev, V. N., Khangulov, S. V., Stadtman, T. C., and Sun, P. D. (1997) *Science 275*, 1305−1308.
37. Trieber, C. A., Rothery, R. A., and Weiner, J. H. (1994) *J. Biol. Chem. 269*, 7103−7109.
38. Schindelin, H., Kisker, C., Hilton, J., Rajagopalan, K. V., and Rees, D. C. (1996) *Science 272*, 1615−1621.
39. Romao, M. J., Archer, M., Moura, I., Moura, J. J., LeGall, J., Engh, R., Schneider, M., Hof, P., and Huber, R. (1995) *Science 270*, 1170−1176.
40. Schneider, F., Lowe, J., Huber, R., Schindelin, H., Kisker, C., and Knablein, J. (1996) *J. Mol. Biol. 263*, 53−69.
41. Axley, M. J., Bock, A., and Stadtman, T. C. (1991) *Proc. Natl. Acad. Sci. U.S.A. 88*, 8450−8454.

BI972858F